AGU PUBLICATIONS

Water Resources Research

RESEARCH ARTICLE

10.1002/2016WR018959

Key Points:

- A Bayesian approach to a nonstationary, bivariate probabilistic model, including the estimation of copula parameters is developed
- The return period of the recent drought varies from approximately 667 to 2652 years under nonstationary assumption.
- The return period of the severity of the recent drought given its 4 year duration is estimated to be nearly 21,000 years.

Supporting Information:

- Table S1-S2

Correspondence to:
H.-H. Kwon,
hkwon@jbnu.ac.kr

Citation:
Kwon, H.-H., and U. Lall (2016), A copula-based nonstationary frequency analysis for the 2012–2015 drought in California, *Water Resour. Res.*, *52*, 5662–5675, doi:10.1002/2016WR018959.

Received 21 MAR 2016
Accepted 1 JUL 2016
Accepted article online 4 JUL 2016
Published online 31 JUL 2016

A copula-based nonstationary frequency analysis for the 2012–2015 drought in California

Hyun-Han Kwon[1,2] and Upmanu Lall[2,3]

[1]Department of Civil Engineering, Chonbuk National University, South Korea, [2]Columbia Water Center, Columbia University, New York, New York, USA, [3]Department of Earth and Environmental Engineering, Columbia University, New York, New York, USA

Abstract Using a multicentury reconstruction of drought, we investigate how rare the 2012–2015 California drought is. A Bayesian approach to a nonstationary, bivariate probabilistic model, including the estimation of copula parameters is used to assess the time-varying return period of the current drought. Both the duration and severity of drought exhibit similar multicentury trends. The period from 800 to 1200 A.D. was perhaps more similar to the recent period than the period from 1200 to 1800 A.D. The median return period of the recent drought accounting for both duration and severity, varies from approximately 667–2652 years, if the model parameters from the different time periods are considered. However, we find that the recent California drought is of unprecedented severity, especially given the relatively modest duration of the drought. The return period of the severity of the recent drought given its 4 year duration is estimated to be nearly 21,000 years.

1. Introduction

Western North America (WNA) has experienced prolonged exposure to concurrent extreme low precipitation and warmer temperatures since the winter of 2011–2012 until 2015 [*AghaKouchak et al.*, 2014; *Devineni et al.*, 2015; *Diaz and Wahl*, 2015; *Griffin and Anchukaitis*, 2014; *Mao et al.*, 2015; *Seager et al.*, 2014; *Swain et al.*, 2014]. Regions of the WNA have undergone periodic decadal-scale severe droughts including the events during the 1930s Dust Bowl, and repeatedly during the early 2000s [*Cook et al.*, 2009; *Cook et al.*, 2014a; *Seager and Hoerling*, 2014; *Seager et al.*, 2007; *Woodhouse et al.*, 2010]. Specifically, California has been characterized by periodic drought and evidence of cyclical megadrought that lasted nearly a decade between 900 and 1300 A.D. as identified in paleoclimate studies [*Cook et al.*, 2010, 2015 *Griffin and Anchukaitis*, 2014; *MacDonald*, 2007; *Schimmelmann et al.*, 2003]. Many studies have confirmed that the ongoing California drought corresponds to an extremely severe condition relative to both the instrumental historical record and paleoclimate reconstructions of hydrologic variables (e.g., PDSI and precipitation) [*Diaz and Wahl*, 2015; *Griffin and Anchukaitis*, 2014; *Mao et al.*, 2015]. Recent studies based on tree rings from blue oaks suggests that the current drought may be the most extreme in terms of severity since the year 800 [*Griffin and Anchukaitis*, 2014; *Robeson*, 2015].

The causes of the drought have generated a great deal of controversy [*Cook et al.*, 2010; *Mao et al.*, 2015]. Some studies suggest the warming climate plays an important role in exacerbating drought condition in WNA [*Cook et al.*, 2014b; *Delworth et al.*, 2015; *Diffenbaugh et al.*, 2015; *Mann and Gleick*, 2015] while the role of climate variability as a main driver of the recent drought are supported by others [*Cheng et al.*, 2016; *Hartmann*, 2015; *Mao et al.*, 2015; *Seager and Hoerling*, 2014; *Seager et al.*, 2014; *Wang and Schubert*, 2014]. A recent study indicated that the current drought was mostly the result of natural variability and modestly exacerbated by warming condition [*Williams et al.*, 2015]. An anomalous high-amplitude ridge pattern has been also discussed as a linkage of the megadroughts in the WNA area [*Wang and Schubert*, 2014; *Wang et al.*, 2014]. The persistent circulation anomaly associated with the ridge pattern centered on the west/southwest coast is associated with low precipitation and high temperature, and hence with regional drought [*Cook et al.*, 2014a; *Wang et al.*, 2014].

Some statistical aspects of the current 2012–2015 drought including extreme value analysis have been investigated by *AghaKouchak et al.* [2014]; *Diaz and Wahl* [2015]; *Griffin and Anchukaitis* [2014]; and *Robeson*

[2015]. Here, a formal nonstationary approach for the estimation of the joint return period of drought variables (i.e., duration and severity) and the uncertainty associated with such estimates is developed. Our focus is on quantifying the time-varying joint probabilities of the severity and duration of the drought, to get an empirical understanding of the rarity of the drought in terms of these metrics, and also its paleoclimate context. The Palmer Drought Severity Index (PDSI) averaged over California using instrumental and tree ring reconstructed paleo climate from 800 to 2015 A.D. is used. Specifically, we explore how likely such a drought would have been over different periods covering the 1200 years of historical record, considering a time-varying bivariate probability of the duration and the severity of the drought. We use Bayesian methods to build a nonstationary, bivariate probabilistic model that considers the covariation of drought duration and severity, and use it to estimate the variation in the return period of the current drought as a function of time. The joint probabilities of the duration and severity of the anomaly are modeled using copulas in a Bayesian estimation framework, that relies on both the historical and the reconstructed paleoclimate record for California.

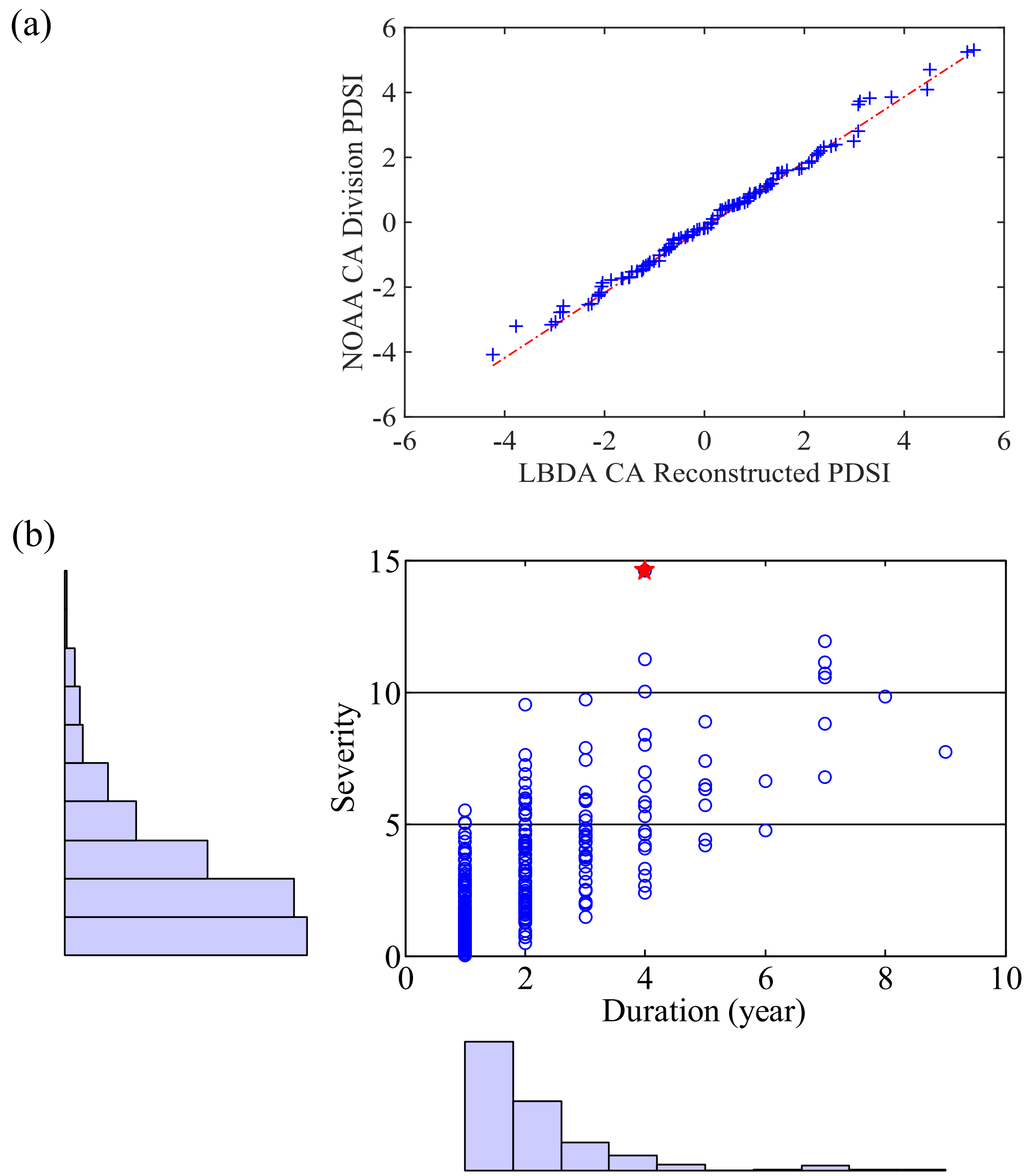

Figure 1. (a) Q-Q plot between LBDA reconstructed PDSI and NOAA CA division PDSI data from 1895 to 2015. (b) Scatter plot of duration and severity based on Paleo (800∼1894) + Observed JJA (1895 + 2015) PDSI. Symbol "star" indicates current status of the drought.

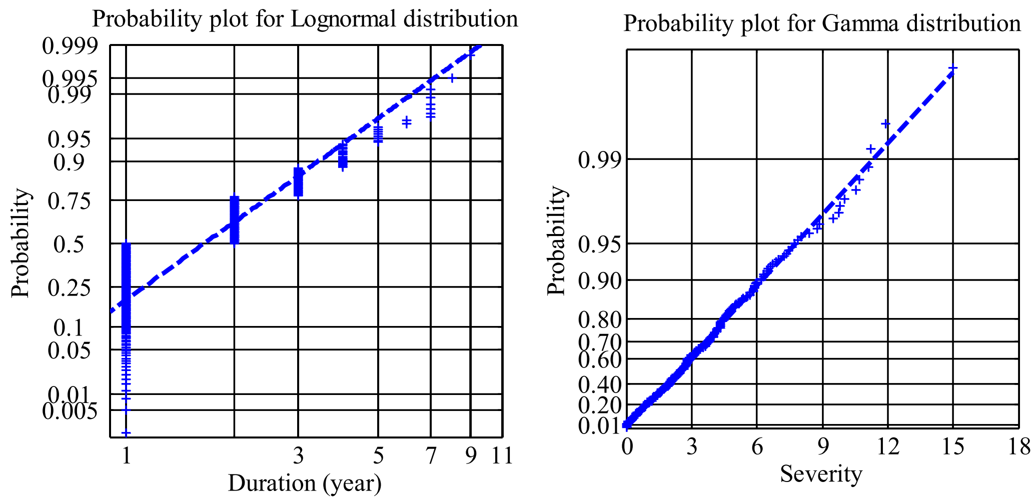

Figure 2. Probability plot for drought duration and severity. Lognormal distribution and Gamma distribution for the duration and the severity are considered as marginal distributions.

2. PDSI Data

We define drought events through PDSI sequences that are continuously negative. The drought ends when PDSI become above 0. We considered the reconstructed PDSI values in the range 32.75°N to 41.75°N and 114.25°W to 124.25°W for 800–2005 from the Living Blended Drought Atlas (LBDA) [*Cook et al.*, 2010], and the reconstructed PDSI data are then clipped to the outline of California. For the current drought data, we extracted California's NOAA climate division PDSI [*Vose et al.*, 2014] data in the same range with the reconstructed data for the analysis. The reconstructed PDSI data were seasonally averaged for June through August (JJA) to better match the instrumental PDSI Data. These two PDSI time series from 1895 to 2005 are highly correlated (r$\sim$0.98). Beyond a correlation of the LBDA and divisional data, a Q-Q plot of these two variables is also represented in Figure 1a. As shown in the Figure 1a, the points in the Q-Q plot lie on a 45° reference line and we assume that the two variables are almost identical. The severity is defined as the cumulative negative PDSI value during the corresponding duration. There are 305 drought events out of 1206 years based on the PDSI. The drought events from the time series of reconstructed PDSI for California are shown in Figure 1b, with the most recent drought identified by a red star.

3. Bayesian Estimation of the Joint Distribution Using Copulas

Copulas [*Lall et al.*, 2016; *Requena et al.*, 2013; *Salvadori and De Michele*, 2004; *Shiau*, 2006] have emerged as a useful tool to model multivariate random variables, since they allow a specification of the marginal distributions of each variable separately from the modeling of their mutual dependence through a copula function. First, the marginal distributions were identified as the lognormal distribution (equation (1)) and the gamma distribution (equation (2)) for drought durations (x) and drought severity (y), respectively, based on goodness-of-fit tests (supporting information Table S1) and graphical evaluation by probability plots as shown in Figure 2.

$$f(x)=\frac{1}{x\sigma\sqrt{2\pi}}e^{-\frac{(\log(x)-\mu_x)^2}{2\sigma^2}} \tag{1}$$

$$f(y)=\frac{y^{k-1}e^{-\tau y}}{\tau^k\Gamma(k)} \tag{2}$$

where, μ_x and σ are the location and scale parameter of the lognormal distribution,; and k and τ are shape and scale parameter of the gamma distribution, respectively.

Here, the Gumbel copula, a member of the family of Archimedean copulas (e.g., Clayton, Frank and Gumbel), defined by one parameter (θ), is chosen by a goodness of fit test (i.e., Deviance Information Criterion, DIC), as summarized in supporting information Table S2. The Gumbel copula is often used for extreme events. A closed functional form is available, and also the copula parameter, θ, can be estimated by using general bivariate dependency measures such as Kendall's rank correlation coefficient and Spearman's rank correlation coefficient. In our work, all parameters, including θ are estimated in a Bayesian framework. The functional form of Gumbel copula is written as follows:

$$C(\mathbf{u},\mathbf{v};\theta)=\exp\left(-\left((-\log(u))^{\theta}+(-\log(v))^{\theta}\right)^{1/\theta}\right) \tag{3}$$

$$u=F_u(x),\ v=F_v(y) \tag{4}$$

where, F_u and F_v are marginal cumulative density function of the two random variables, x and y that are realizations of a random variable X representing drought duration and Y representing drought severity.

A Bayesian approach is used to compute the posterior distribution of the severity and duration of drought, through an estimate of the posterior distribution of the parameters of their marginal distributions and of the copula function. The posterior distribution of the parameter vector, Θ, $p(\Theta|\mathbf{D})$ can be written as follows [*Kwon et al.*, 2008, 2009]:

$$p(\Theta|\mathbf{D})=\frac{p(\Theta)\times p(\mathbf{D}|\Theta)}{p(\mathbf{D})}=\frac{p(\Theta)\times p(\mathbf{D}|\Theta)}{\int p(\Theta)\times p(\mathbf{D}|\Theta)}d\Theta \propto p(\Theta)\times p(\mathbf{D}|\Theta) \tag{5}$$

where Θ is the parameter vector of the distribution to be fitted, $p(\mathbf{D}|\Theta)$ is the likelihood function, $\mathbf{D}$ is the observation vector, and $p(\Theta)$ is the prior distribution. The joint likelihood function for the drought characteristics based on the copula function along with the lognormal and the gamma distribution can be written as equation (6). The prior distributions for five parameters are assumed to be normal (for μ_x), gamma (for σ, k, τ), and uniform distribution (for θ). The likelihood function is then written as:

$$p(\boldsymbol{D}|\boldsymbol{\Theta})=L_G(\boldsymbol{x},\boldsymbol{y};\mu_x,\sigma,k,\tau,\theta) \tag{6}$$

A parametric polynomial regression model for the time-varying parameters of probability density functions is considered. A linear model was initially considered but the DIC favored the polynomial trend model. In the present study, the variance was not found to change significantly as a function of time so that we limit its application to the mean as a time-varying moment. The prior distributions for regression coefficients (i.e., φ and η) are assumed to be normal distribution. The resulting model is formulated as follows:

$$p(\boldsymbol{D}|\boldsymbol{\Theta})=L_G(\boldsymbol{x},\boldsymbol{y};\boldsymbol{\mu_x}(\boldsymbol{t}),\sigma,\boldsymbol{k}(\boldsymbol{t}),\tau,\theta) \tag{7}$$

$$\mu_x(t)=\phi_1+\phi_2 t+\phi_3 t^2+\phi_4 t^3 \tag{8}$$

$$\mu_y(t)=k(t)\times\tau \tag{9}$$

$$k(t)=\eta_1+\eta_2 t+\eta_3 t^2+\eta_4 t^3 \tag{10}$$

$$\phi_{1-4}\sim N\left(0,10^4\right) \tag{11}$$

$$\eta_{1-4}\sim N\left(0,10^4\right) \tag{12}$$

$$\sigma\sim G(0.1,0.1) \tag{13}$$

$$\tau\sim G(0.1,0.1) \tag{14}$$

$$\theta\sim G(0.1,0.1) \tag{15}$$

where, $\boldsymbol{\phi}$ and $\boldsymbol{\eta}$ are regression coefficients for the time-varying parameters $\boldsymbol{\mu_x}$ and $\boldsymbol{\mu_y}$ that are the mean of the lognormal and gamma distribution, respectively.

The joint posterior distribution of the parameter set $\boldsymbol{\Theta}=[\phi,\sigma,\eta,\tau,\theta]$ can be written as equation (16), by substituting the likelihood function as described in equation (7) and the priors (11$\sim$15) into the Bayes theorem (5).

$$p(\Theta|\boldsymbol{D}) \propto p(\Theta)p(\boldsymbol{D}|\Theta) = \prod_{i=1}^{4}\prod_{t=1}^{n} L_G(\boldsymbol{x}(\boldsymbol{t}), \boldsymbol{y}(\boldsymbol{t})|\boldsymbol{\mu_x}(\boldsymbol{t}), \sigma, \boldsymbol{k}(\boldsymbol{t}), \tau, \theta) \times N(\phi_i|0, 10^4) \times G(\sigma|0.1, 0.1) \times N(\eta_i|0, 10^4) \times G(\tau|0.1, 0.1) \times U(\theta|0, 50) \tag{16}$$

A Markov Chain Monte Carlo (MCMC) approach, specifically the Gibbs sampler, was used to sample from the joint posterior distribution. The Gibbs sampler utilizes a specified multidimensional probability density function for obtaining a sequence of observations, by fixing all the parameters except one of the parameters. In other words, the conditional distribution of the parameter is conditioned on the fixed values associated with the other parameters [*Kwon et al.*, 2008]. For the convergence, the Gelman–Rubin (GR) index [*Gelman and Rubin*, 1992] was used, with values less than 1.2 suggesting convergence. The GR index was close to 1.0 for all parameters after 10,000 iterations with a 1000 cycle burn in.

The recurrence interval or return period of drought severity [*Shiau and Shen*, 2001] (T_{DS}) and duration [*Shiau*, 2006] (T_{DD}) can be estimated as follows:

$$T_{DS} = \frac{E(L)}{P(S \geq s)} = \frac{E(L)}{1 - F_S(s)} \tag{17a}$$

$$T_{DD} = \frac{E(L)}{P(D \geq d)} = \frac{E(L)}{1 - F_D(d)} \tag{17b}$$

Here, *E(L)* is the expected value of the time interval between the initiation of successive droughts. [*Shiau*, 2006] proposed a methodology that categorizes the return periods of bivariate distributed hydrologic events as joint and conditional return periods. The joint drought duration and severity return periods can be defined in two cases: return period for $D \geq d$ and $S \geq s$ and return period for $D \geq d$ or $S \geq s$.

$$T_{DDS} = \frac{E(L)}{P(D \geq d, S \geq s)} = \frac{E(L)}{1 - F_D(d) - F_S(s) + C(F_D(d), F_S(s))} \tag{17c}$$

$$T'_{DDS} = \frac{E(L)}{P(D \geq d \quad or \quad S \geq s)} = \frac{E(L)}{1 - C(F_D(d), F_S(s))} \tag{17d}$$

where T_{DDS} denotes the joint return period for $D \geq d$ and $S \geq s$; T'_{DDS} denotes the joint return period for $D \geq d$ or $S \geq s$;. Detailed discussions on the relationships between univariate, bivariate, and conditional return periods can be found in *Shiau* [2006].

A schematic framework of the copula-based nonstationary frequency analysis within the Bayesian framework is illustrated in Figure 3. The proposed approach can be applied to a wider range of hydroclimatic data including the PDSI. The PDSI is readily available and there is a reconstruction of PDSI that is publically available in online databases (e.g., https://www.ncdc.noaa.gov/data-access/paleoclimatology-data). The development of reconstructions of other drought indices [*Cook et al.*, 1999; *Cook et al.*, 2007; *Gou et al.*, 2015; *Li et al.*, 2006], where paleoclimate data may not be readily available, would be useful to connect such analyses more closely to water management.

4. Results

4.1. Parameter Estimation and Model Identification

The Bayesian model is used to develop a posterior density function for each of the parameters of interest using MCMC. The posterior mean and 95% credible interval for a set of parameters along with the DIC values are summarized in Table 1. We see that the parameters in both stationary (S1) and nonstationary models (N1 and N2) are in general significant since the posterior distributions are not centered about a value of zero and the uncertainty range is also relatively tight. In the nonstationary model using the polynomial regression approach (N2), the regression coefficients associated with the severity ($\boldsymbol{\eta}$) appear to be more consistent than those for duration ($\boldsymbol{\phi}$) since their signs do not change over time. The posterior distributions of the model parameters for both the stationary and the nonstationary case are illustrated in Figure 4–6, respectively.

For the identification of the nonstationary model, the DIC was considered. The DIC is a statistical measure for Bayesian model comparison in hierarchical modeling that is a generalization of the AIC (Akaike

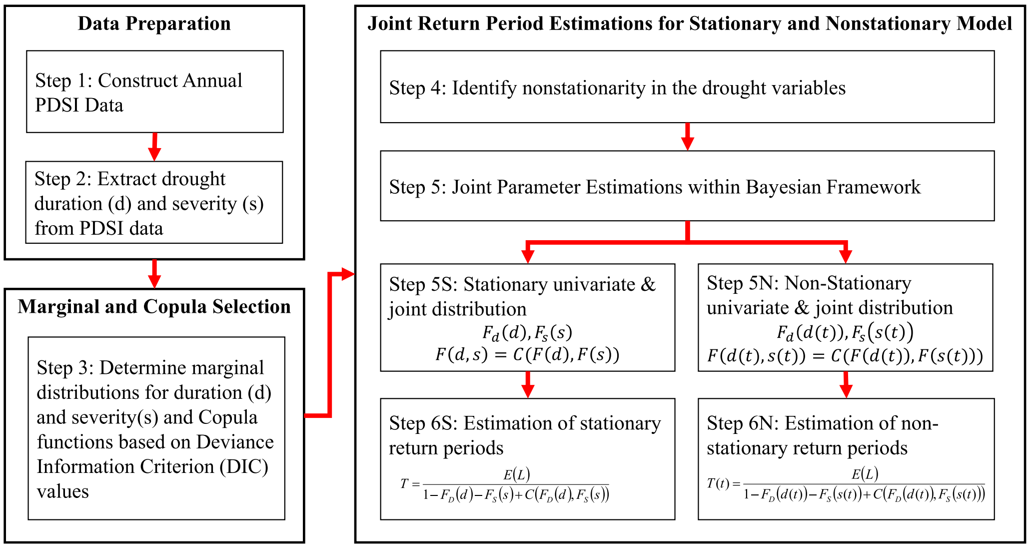

Figure 3. A schematic framework of the copula-based nonstationary drought frequency analysis within the Bayesian framework.

information criterion) and BIC (Bayesian information criterion). The lower the DIC value, the better the model fits the data. The nonstationary model is better than the stationary model given the DIC as shown in Table 1. The difference, however, is relatively small. As noted earlier, we also considered a parametric linear regression model for the time-varying parameters of probability density functions for the duration and severity. Although the parameters for the linear model are all significant, the DIC (or log-likelihood) is almost identical to that of the stationary model which is about 1922.3 (or −958.4). The nonstationary copula model with the polynomial regression model was the best one based on the DIC. Thus, this study uses the polynomial regression model as the best fit model for subsequent analysis. The implications for the assessment of the return period of the current drought are discussed in the next section. The results from the stationary and the nonstationary models are summarized and compared in the following sections.

4.2. Stationary Bivariate Frequency Analysis

First consider the recurrence intervals of the duration and severity of the 2012–2015 drought based on the stationary model. The univariate return periods and their 95% posterior credible interval for the current drought (2012–2015) duration and severity, as estimated from the equations (17a) and (17b), are 59 (48–73)

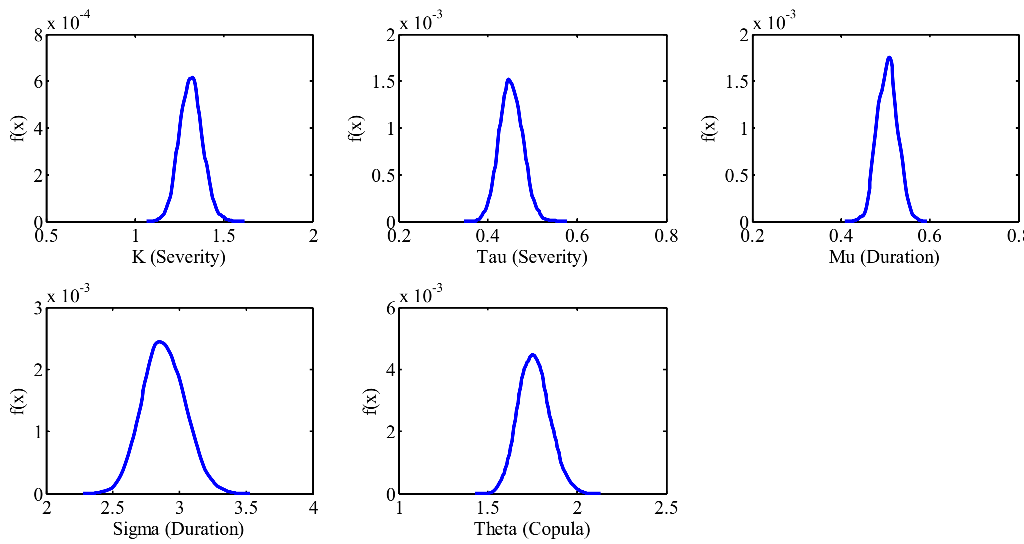

Figure 4. Marginal posterior density functions for parameters of stationary Gumbel copula (S1).

10.1002/2016WR018959

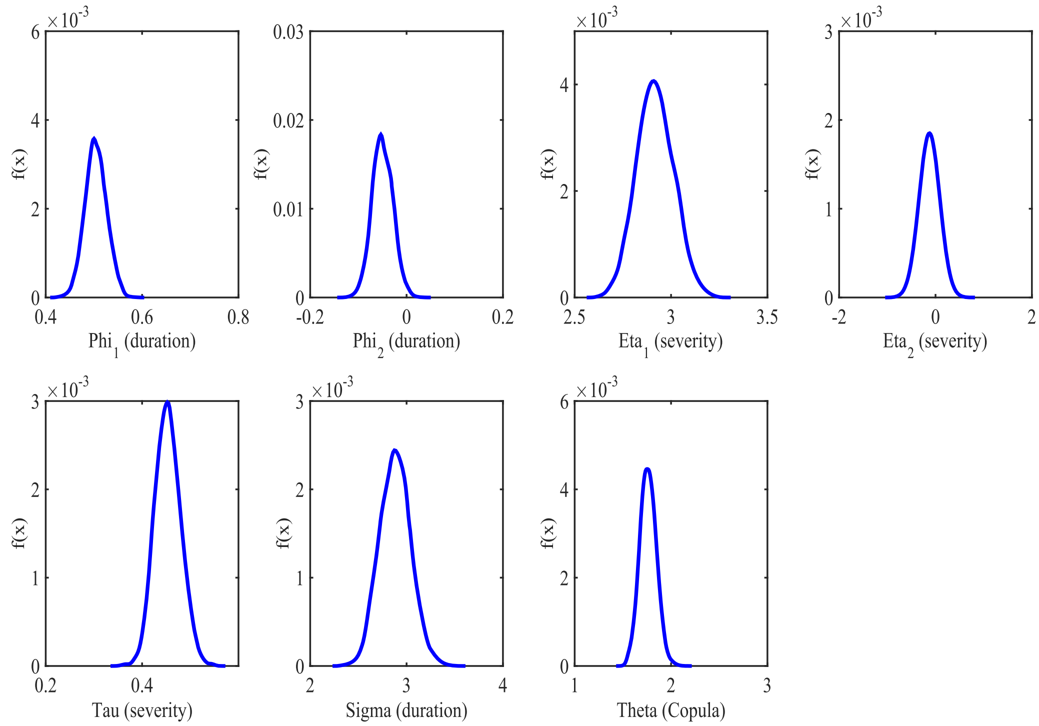

Figure 5. Marginal posterior density functions for parameters of nonstationary Gumbel copula with linear regression model (N1).

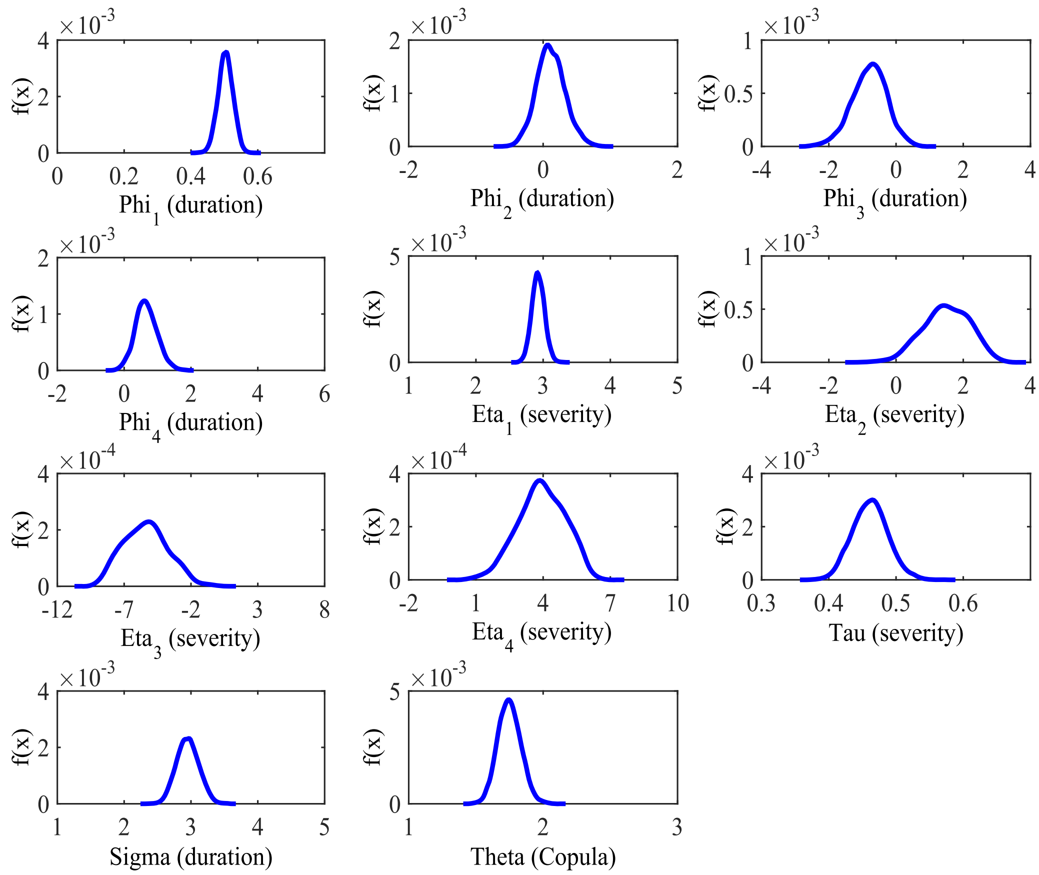

Figure 6. Marginal posterior density functions for parameters of nonstationary Gumbel copula with polynomial regression model (N2).

Table 1. Estimated Parameters and Associated Uncertainty of the Copula-Based Drought Analysis Model[a]

Copula Model				2.50%	50%	97.50%	Log-likelihood	Total Log-likelihood	DIC
S1	Lognormal	μ		0.462	0.505	0.549	−413.00	−959.27	1923.10
		σ		2.588	2.879	3.201			
	Gamma	k		1.193	1.314	1.446	−633.50		
		τ		0.404	0.451	0.506			
	Copula	θ		1.598	1.756	1.938	87.43		
N1	Lognormal	μ	ϕ_1	0.460	0.504	0.549	−412.60		
			ϕ_2	−0.091	−0.051	−0.007			
		σ		2.581	2.881	3.201			
	Gamma	k	η_1	2.737	2.916	3.109	−633.40	−958.40	1922.3
			η_2	−0.285	−0.127	0.030			
		τ		0.404	0.453	0.507			
	Copula	θ		1.600	1.761	1.936	87.60		
N2	Lognormal	μ	φ_1	0.460	0.504	0.546	−410.40		1918.31
			φ_2	−0.291	0.104	0.558			
			φ_3	−1.867	−0.765	0.186			
			φ_4	0.053	0.646	1.349			
		σ		2.637	2.949	3.278			
	Gamma	k	η_1	2.745	2.925	3.118	−630.70	−955.39	
			η_2	0.140	1.505	2.713			
			η_3	−8.234	−5.381	−2.238			
			η_4	1.870	3.937	5.748			
		τ		0.412	0.462	0.515			
	Copula	θ		1.588	1.747	1.921	85.71		

[a]S1 is the stationary copula model while N1 and N2 are the nonstationary models using the linear and polynomial regression model for the mean.

and 1371 (846–2353) years, respectively. The expected drought interval time between successive events, *E(L)*, is about 4 years. The current 4 year drought duration (i.e., from 2012 to 2015) is not long enough to be regarded as a megadrought in California while the drought severity is exceptionally high reaching a millennium-scale megadrought.

Second, we investigated joint return periods for (duration and severity, $D \geq d$ and $S \geq s$) and (duration or severity, $D \geq d$ or $S \geq s$) using equations (17c) and (17d). As illustrated in Figure 7, the "AND" joint return period T_{DDS} for the current drought is nearly 1500 [897–2464] years—larger than the univariate return periods. Note that there is an inequality between univariate return period and joint return period [*Requena et al.*, 2013; *Salvadori and De Michele*, 2004] as follows: $T'_{DDS} \leq \min\left[T_{DD}, T_{DS}\right] \leq \max\left[T_{DD}, T_{DS}\right] \leq T_{DDS}$. The drought severity index ($\sim$14.59), for the current 4 year drought is even worse than those recorded for the more prolonged droughts (e.g., 5–9 year duration) identified from paleo PDSI data. Consequently, the

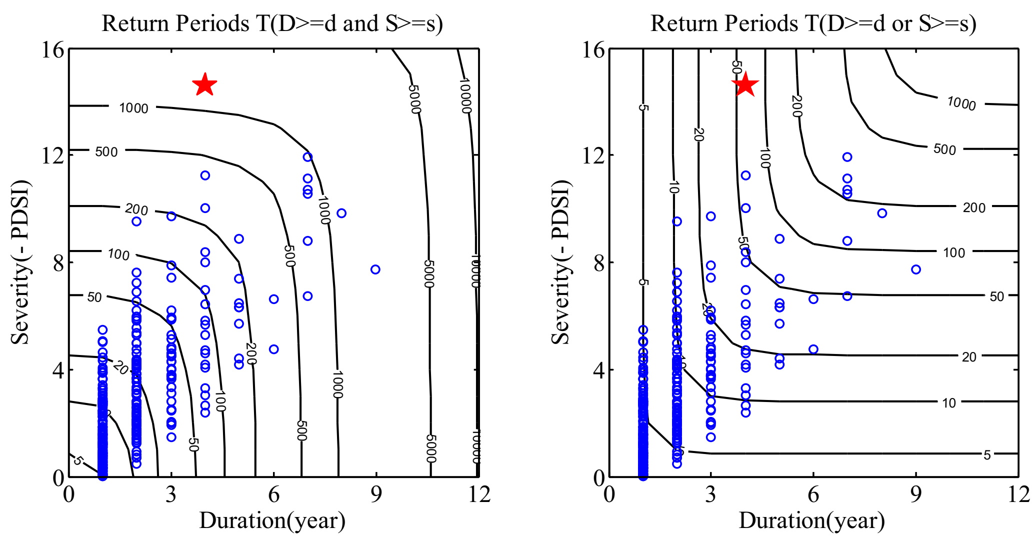

Figure 7. Stationary model based joint return periods between duration and severity using median values of parameters.

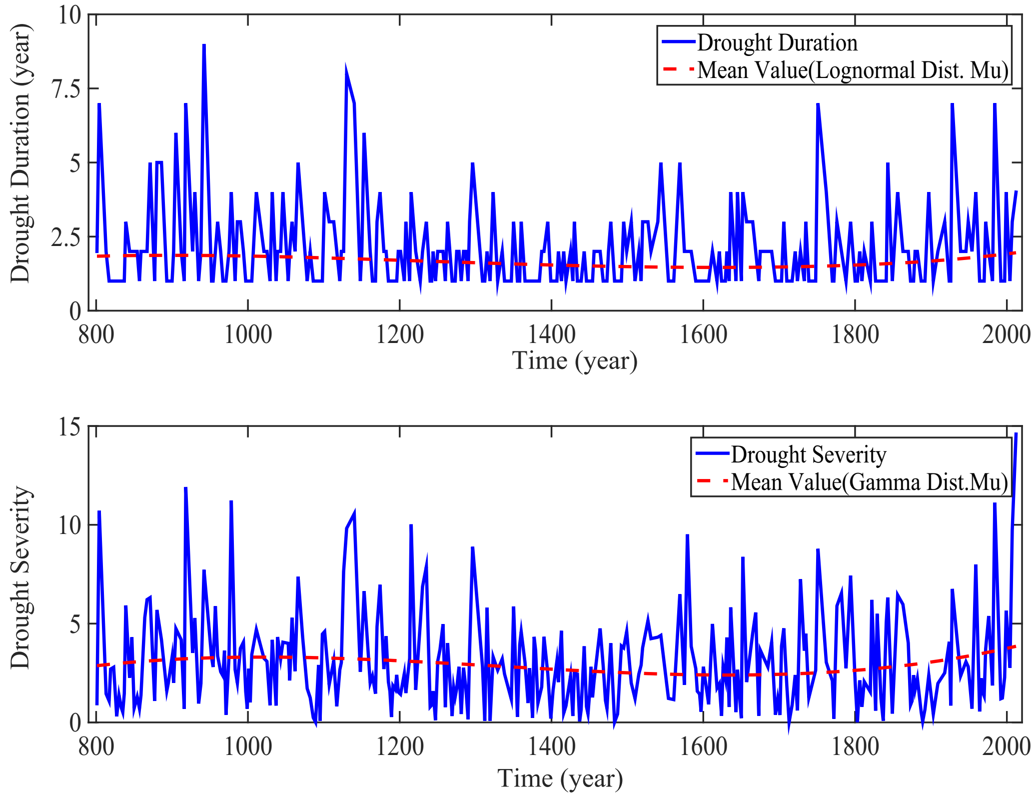

Figure 8. A polynomial trend of parameter for drought duration and severity. The red-dotted line is the mean value of the Lognormal and Gamma distribution for duration and severity, respectively.

higher assignment of the joint return period is not a surprise. For a drought of this duration, the severity is unprecedented. The estimated conditional return period of drought severity given a duration of 4 years is greater than 21,580 [11,719–41,957] years.

4.3. Nonstationary Bivariate Frequency Analysis

Let us now consider time-varying return periods for (i) the duration, (ii) the severity, (iii) the duration and the severity, and (iv) the duration or the severity of the 2012–2015 California drought. For all four measures, we find that there are polynomial trends in drought occurrence.

The recent drought appears to correspond to a period similar to relatively frequent droughts during the period 800–1200 A.D., as opposed to the period 1200–1600 A.D. which was relatively drought free as shown in Figure 8. Based on the estimated time-varying parameters, time-varying return periods of duration and severity for the 2012–2015 California drought are estimated and illustrated in Figure 9. The assessment that the duration is not at all unusual, but the severity is unusual both by itself and jointly with duration is reinforced.

As a complement, the drought duration and severity with 5%, 1%, and 0.2% probability of exceedance in a given year (corresponding to 20, 100, and 500 year recurrence intervals) for each year over the last 1200 years, was also estimated. These results along with the drought duration and severity time series, and the uncertainty of estimation from the Bayesian model are shown in Figure 10. The nonstationary model based joint return periods between duration and severity using the median parameters for the year 2015 are also illustrated in Figure 11.

While, an increasing trend in drought severity and duration is indicated in the most recent period, accounting for the uncertainty of estimation, the return periods of the current drought's indicators are statistically indistinguishable from those for a time stationary model fit to the full 1200 year record. Specifically, the estimated return period of the current events severity and duration are 1443 [897–2464], 1059 [653, 1794], 2631 [1476, 4900], and 667 [359, 1348] years, for the stationary model, and for the model parameters

10.1002/2016WR018959

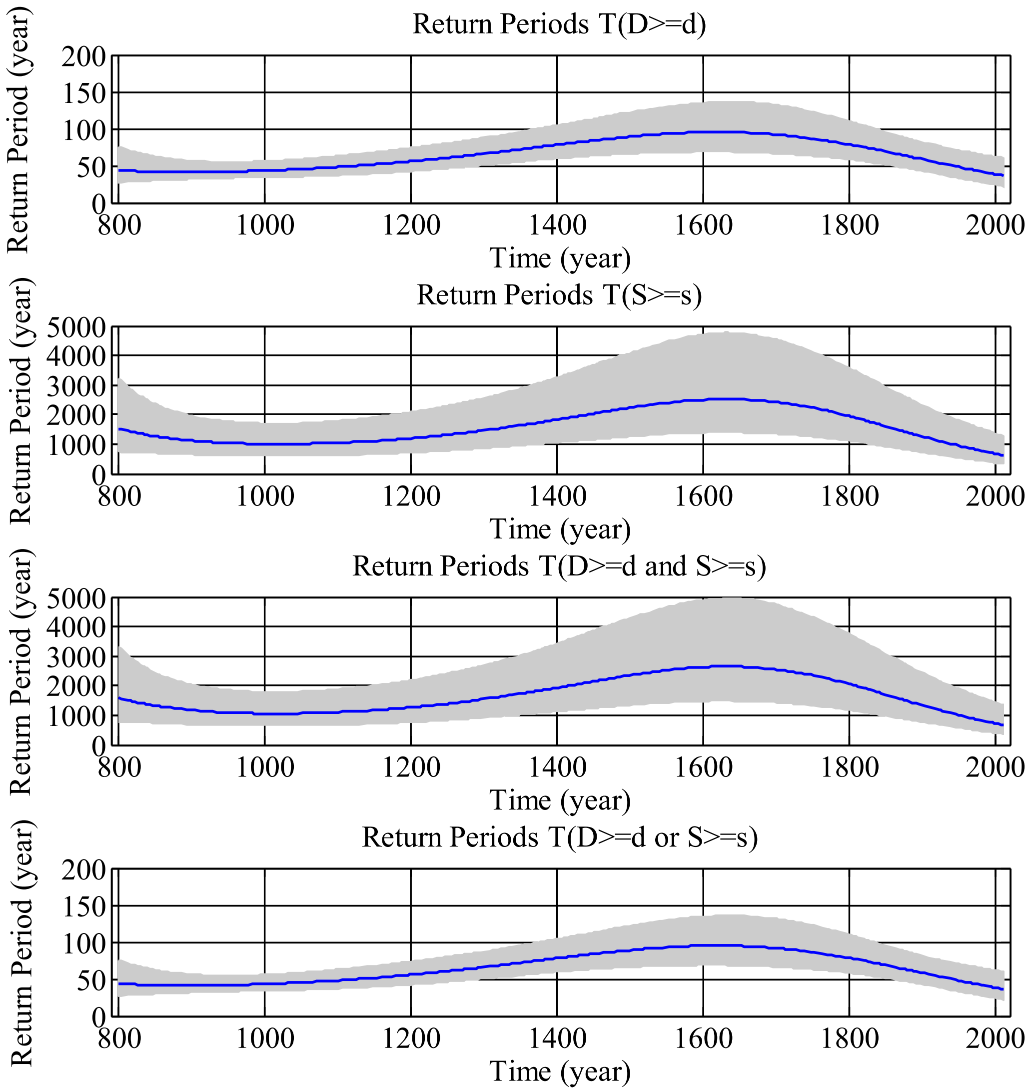

Figure 9. The univariate return periods of (a) duration and (b) severity equal to or greater than the 2012–2015 California drought d and s. The bivariate joint return periods (c) T_{and} and (d) T_{or} with duration and severity equal to or greater than the 2012–2015 California drought d and s. Credible intervals (2.5% and 97.5%) for the return periods are described by shaded area.

corresponding to the years 1000, 1600, and 2015 A.D., respectively, covering the three regimes identified in the nonstationary model.

5. Discussion

The primary contribution of this paper is the development and application of the nonstationary Bayesian model for the estimation of the joint probability of recurrence of a drought with a specified duration and severity, and the uncertainty associated with such estimates. The findings of our analyses for California are broadly consistent with those reported in the literature. Even accounting for estimation uncertainty in the Bayesian framework, the recent California drought is of unprecedented severity, especially for the duration of the drought (which by itself is not at all remarkable). While the difference between the stationary and nonstationary models is not large based on the statistical criteria, again consistent with the past literature, we identify that the period from 800 to1200 A.D. was perhaps more similar to the recent period than the period from 1200 to 1800 A.D. when droughts of high duration and severity were not as frequent. Even so, the median return period of the current drought in terms of duration and severity (T_{DDS}**)**, varies from approximately 667 (i.e., year-2015) to 2652 (i.e., year-1634) years, if the model parameters from the different

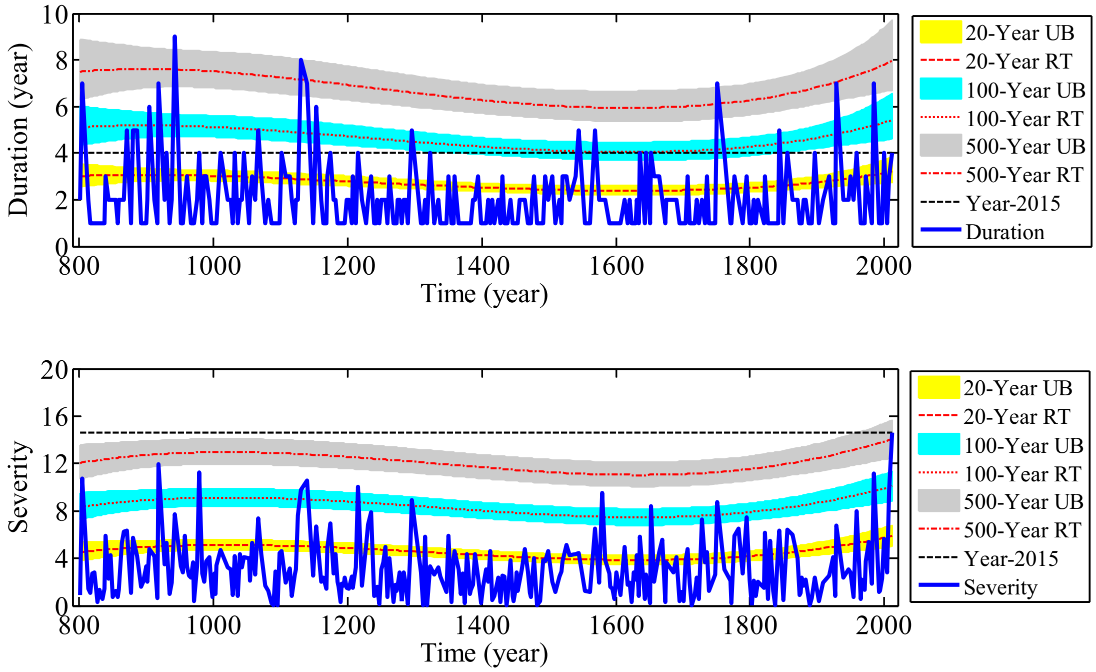

Figure 10. Estimates of the drought duration and severity with 5%, 1%, and 0.2% probability of occurring in a given year (i.e., 20, 100, and 500 year drought) for each year. Red-dotted lines show the nonstationary estimates of the 20, 100, and 500 year droughts based on time-varying parameters, and their credible intervals (2.5% and 97.5%) are described by shaded area.

time periods are considered. In all cases, it is the severity of the drought that stands out, rather than the duration, although both exhibit broadly similar trends. Using the most recent parameters, the return period based on the recent time period is indeed the lowest in the record.

The argument in *Cook et al.* [2015]; *Cook et al.* [2010]; *Griffin and Anchukaitis* [2014]; *MacDonald* [2007]; *Schimmelmann et al.* [2003] that the contribution of the warmer temperatures leads to the higher stress indicated in the PDSI is notable in this regard. However, the counter argument that the state of ENSO, specifically, the persistent La Nina event over the last several years may play role is also worth considering. An obvious reconciliation of the two arguments is that the ENSO state is associated with the occurrence and duration of the drought, and the unusual warming of the recent period accentuates the severity of the

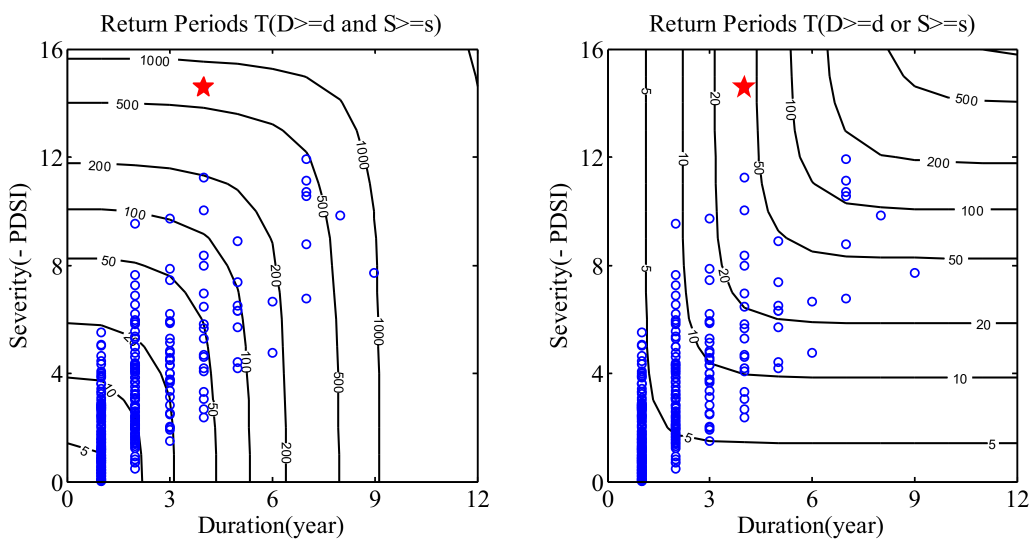

Figure 11. Nonstationary model-based joint return periods between duration and severity using the median parameters for the year 2015.

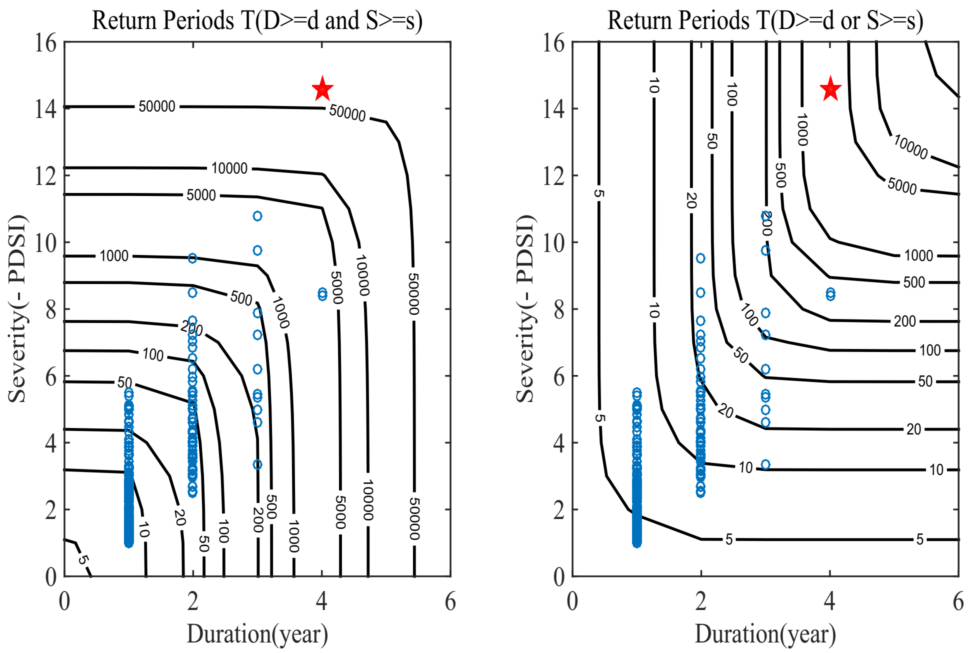

Figure 12. Nonstationary model-based joint return periods between duration and severity using the median parameters for the year 2015. Here, a different threshold, PDSI<-1, is used to define drought.

drought as measured by the PDSI. We expect that in future work we will explore the use of the proposed model to predict extreme drought in performance with a different set of predictors over a longer period of record.

One concern that could be raised with our analysis is that the duration considered was for any period with PDSI continuously below 0. Consequently, we also considered a definition of drought such that the PDSI is continuously below −1. This would possibly censor minor excursions and thus provide an assessment of droughts that are of greater concern. The results of this analysis for the nonstationary model are provided in Figure 12. We can see that the return periods for the joint occurrence or for the duration or severity being as extreme as for the recent drought are much greater under this analysis, reinforcing the extreme nature of the recent event.

A recent effort [*Ho et al*., 2016] to reconstruct streamflow records from the Living Blended Drought Atlas, which contains a PDSI reconstruction was presented for the Missouri River Basin, and has now been extended to cover 3224 USGS stream gages. Streamflow reconstruction skill is shown to be higher in regions where the PDSI reconstruction skill was higher. The argument advanced is that the tree rings, the PDSI, and streamflow represent different transfer functions for the climate input. However, at least at the annual scale, it is possible to relate the estimates of PDSI from tree rings to estimates of streamflow. In essence, for persistent drought, there is some correspondence between the timing and intensity of these events.

On the other hand, it should be noted that meteorological drought indices such as the PDSI, or the SPI are not directly comparable to specific hydrologic variables such as discharge, snowpack, and reservoir storage. Further, usual drought indices including the PDSI do not consider various aspects of supply and demand, thus, it may not be appropriate to use existing drought indices for water resources management [*Devineni et al*., 2015]. In this regard, new indices to estimate drought-induced water stress using current daily water demands and supply data have been introduced and applied at the country level in the USA [*Devineni et al*., 2015; *Lall et al*., 2016].

It has been well-documented that hydrologic variables often exhibit nonstationarity, characterized by the secular trends and periodically time-varying moments due to the effect of low-frequency climate [*Jain and Lall*, 2000, 2001]. In a changing climate, an extension of the stationary drought frequency analysis into nonstationary one could lead to constructive water resources management framework that can better target where dynamic drought risk assessment is needed. Some implications of this study on the water resources management are summarized as follows. First, understanding changes in the risk of persistent drought may allow us to better manage evolutionary uncertainty associated with climate variability. Second, the use of dynamic risk information could be directly or indirectly tied to attempts to reduce uncertainty in the estimation of the drought risk, leading to reduction in the potential costs of water storage structures for some future hydrologic designs. This is particularly true when climate variability and climate change are concerned.

Acknowledgments
The first author was supported by a grant (15RDRP-B076564-02) from Regional Development Research Program funded by Ministry of Land, Infrastructure and Transport of Korean government. The second author was supported by the U.S. National Science Foundation, under grant EAR-1360446. The data used in this study are available upon request from the corresponding author via email (hkwon@jbnu.ac.kr).

References

AghaKouchak, A., L. Cheng, O. Mazdiyasni, and A. Farahmand (2014), Global warming and changes in risk of concurrent climate extremes: Insights from the 2014 California drought, *Geophys. Res. Lett.*, *41*, 8847–8852, doi:10.1002/2014GL062308.

Cheng, L., M. Hoerling, A. AghaKouchak, B. Livneh, X.-W. Quan, and J. Eischeid (2016), How has human-induced climate change affected California drought risk?, *J. Clim.*, *29*(1), 111–120.

Cook, B. I., R. L. Miller, and R. Seager (2009), Amplification of the North American "Dust Bowl" drought through human-induced land degradation, *Proc. Natl. Acad. Sci. U. S. A.*, *106*(13), 4997–5001.

Cook, B. I., R. Seager, and J. E. Smerdon (2014a), The worst North American drought year of the last millennium: 1934, *Geophys. Res. Lett.*, *41*, 7298–7305, doi:10.1002/2014GL061661.

Cook, B. I., J. E. Smerdon, R. Seager, and S. Coats (2014b), Global warming and 21st century drying, *Clim. Dyn.*, *43*(9–10), 2607–2627.

Cook, B. I., T. R. Ault, and J. E. Smerdon (2015), Unprecedented 21st century drought risk in the American Southwest and Central Plains, *Sci. Adv.*, *1*(1).

Cook, E. R., D. M. Meko, D. W. Stahle, and M. K. Cleaveland (1999), Drought reconstructions for the continental United States, *J Clim.*, *12*(4), 1145–1162.

Cook, E. R., R. Seager, M. A. Cane, and D. W. Stahle (2007), North American drought: Reconstructions, causes, and consequences, *Earth Sci. Rev.*, *81*(1), 93–134.

Cook, E. R., R. Seager, R. R. Heim, C. Herweijer, R. S. Vose, and C. Woodhouse (2010), Megadroughts in North America: Placing IPCC projections of hydroclimatic change in a long-term palaeoclimate context, *J. Quat. Sci.*, *25*(1), 48–61.

Delworth, T. L., F. Zeng, A. Rosati, G. A. Vecchi, and A. T. Wittenberg (2015), A link between the hiatus in global warming and North American drought, *J Clim.*, *28*(9), 3834–3845.

Devineni, N., U. Lall, E. Etienne, D. Shi, and C. Xi (2015), America's water risk: Current demand and climate variability, *Geophys. Res. Lett.*, *42*, 2285–2293, doi:10.1002/2015GL063487.

Diaz, H. F., and E. R. Wahl (2015), Recent California water year precipitation deficits: A 440-year perspective, *J Clim.*, *28*(12), 4637–4652.

Diffenbaugh, N. S., D. L. Swain, and D. Touma (2015), Anthropogenic warming has increased drought risk in California, *Proc. Natl. Acad. Sci. U. S. A.*, *112*(13), 3931–3936.

Gelman, A., and D. B. Rubin (1992), Inference from iterative simulation using multiple sequences, *Stat. Sci.*, *7*(4), 457–472.

Gou, X., Y. Deng, L. Gao, F. Chen, E. Cook, M. Yang, and F. Zhang (2015), Millennium tree-ring reconstruction of drought variability in the eastern Qilian Mountains, northwest China, *Clim. Dyn.*, *45*(7-8), 1761–1770.

Griffin, D., and K. J. Anchukaitis (2014), How unusual is the 2012–2014 California drought?, *Geophys. Res. Lett.*, *41*, 9017–9023, doi:10.1002/2014GL062433.

Hartmann, D. L. (2015), Pacific sea surface temperature and the winter of 2014, *Geophys. Res. Lett.*, *42*, 1894–1902, doi:10.1002/2015GL063083.

Ho, M., Lall, U. and Cook, E. R. (2016), Can a paleo-drought record be used to reconstruct streamflow? A case-study for the Missouri River Basin, *Water Resour. Res.*, doi:10.1002/2015WR018444, in press.

Jain, S., and U. Lall (2000), Magnitude and timing of annual maximum floods: Trends and large-scale climatic associations for the Blacksmith Fork River, Utah, *Water Resour. Res.*, *36*(12), 3641–3651.

Jain, S., and U. Lall (2001), Floods in a changing climate: Does the past represent the future?, *Water Resour. Res.*, *37*(12), 3193–3205.

Kwon, H.-H., C. Brown, and U. Lall (2008), Climate informed flood frequency analysis and prediction in Montana using hierarchical Bayesian modeling, *Geophys. Res. Lett.*, *35*, L05404, doi:10.1029/2007GL032220.

Kwon, H. H., U. Lall, and J. Obeysekera (2009), Simulation of daily rainfall scenarios with interannual and multidecadal climate cycles for South Florida, *Stoch. Environ. Res. Risk A*, *23*(7), 879–896.

Lall, U., N. Devineni, and Y. Kaheil (2016), An empirical, nonparametric simulator for multivariate random variables with differing marginal densities and nonlinear dependence with hydroclimatic applications, *Risk Anal.*, *36*(1), 57–73.

Li, J., X. Gou, E. R. Cook, and F. Chen (2006), Tree-ring based drought reconstruction for the central Tien Shan area in northwest China, *Geophys. Res. Lett.*, *33*, L07715, doi:10.1029/2006GL025803.

MacDonald, G. M. (2007), Severe and sustained drought in southern California and the West: Present conditions and insights from the past on causes and impacts, *Quat. Int.*, *173*, 87–100.

Mann, M. E., and P. H. Gleick (2015), Climate change and California drought in the 21st century, *Proc. Natl. Acad. Sci. U. S. A.*, *112*(13), 3858–3859.

Mao, Y., B. Nijssen, and D. P. Lettenmaier (2015), Is climate change implicated in the 2013–2014 California drought? A hydrologic perspective, *Geophys. Res. Lett.*, *42*, 2805–2813, doi:10.1002/2015GL063456.

Requena, A., L. Mediero Orduña, and L. Garrote de Marcos (2013), A bivariate return period based on copulas for hydrologic dam design: Accounting for reservoir routing in risk estimation, *Hydrol. Earth Syst. Sci.*, *17*(8), 3023–3038.

Robeson, S. M. (2015), Revisiting the recent California drought as an extreme value, *Geophys. Res. Lett.*, *42*, 6771–6779, doi:10.1002/2015GL064593.

Salvadori, G., and C. De Michele (2004), Frequency analysis via copulas: Theoretical aspects and applications to hydrological events, *Water Resour. Res.*, *40*, W12511, doi:10.1029/2004WR003133.

Schimmelmann, A., C. B. Lange, and B. J. Meggers (2003), Palaeoclimatic and archaeological evidence for a 200-yr recurrence of floods and droughts linking California, Mesoamerica and South America over the past 2000 years, *Holocene*, *13*(5), 763–778.

Seager, R., and M. Hoerling (2014), Atmosphere and ocean origins of North American droughts*, *J Clim.*, *27*(12), 4581–4606.

Seager, R., M. Ting, I. Held, Y. Kushnir, J. Lu, G. Vecchi, H.-P. Huang, N. Harnik, A. Leetmaa, and N.-C. Lau (2007), Model projections of an imminent transition to a more arid climate in southwestern North America, *Science*, *316*(5828), 1181–1184.

Seager, R., M. Hoerling, S. Schubert, H. Wang, B. Lyon, A. Kumar, J. Nakamura, and N. H. Henderson (2014), Causes and predictability of the 2011-14 California Drought, assessment report, NOAA, Md.

Shiau, J. T. (2006), Fitting drought duration and severity with two-dimensional copulas, *Water Resour. Manage.*, *20*(5), 795–815.

Shiau, J.-T., and H. W. Shen (2001), Recurrence analysis of hydrologic droughts of differing severity, *J. Water Resour. Plann. Manage.*, *127*(1), 30–40.

Swain, D. L., M. Tsiang, M. Haugen, D. Singh, A. Charland, B. Rajaratnam, and N. S. Diffenbaugh (2014), The extraordinary California drought of 2013-2014: Character, context, and the role of climate change, *Bull. Am. Meteorol. Soc.*, *95*(7), S3–S7.

Vose, R. S., S. Applequist, M. Squires, I. Durre, M. J. Menne, C. N. Williams Jr., C. Fenimore, K. Gleason, and D. Arndt (2014), Improved historical temperature and precipitation time series for US climate divisions, *J. Appl. Meteorol. Climatol.*, *53*(5), 1232–1251.

Wang, H., and S. Schubert (2014), Causes of the extreme dry conditions over California during early 2013, *Bull. Am. Meteorol. Soc.*, *95*(7), S7–S11.

Wang, S. Y., L. Hipps, R. R. Gillies, and J. H. Yoon (2014), Probable causes of the abnormal ridge accompanying the 2013–2014 California drought: ENSO precursor and anthropogenic warming footprint, *Geophys. Res. Lett.*, *41*, 3220–3226, doi:10.1002/2014GL059748.

Williams, A. P., R. Seager, J. T. Abatzoglou, B. I. Cook, J. E. Smerdon, and E. R. Cook (2015), Contribution of anthropogenic warming to California drought during 2012–2014, *Geophys. Res. Lett.*, *42*, 6819–6828, doi:10.1002/2015GL064924.

Woodhouse, C. A., D. M. Meko, G. M. MacDonald, D. W. Stahle, and E. R. Cook (2010), A 1,200-year perspective of 21st century drought in southwestern North America, *Proc. Natl. Acad. Sci. U. S. A.*, *107*(50), 21,283–21,288.